

A Robust, Freezing-resistant and Highly Ion Conductive Ionogel Electrolyte towards Lithium Metal Batteries Workable at -30 °C

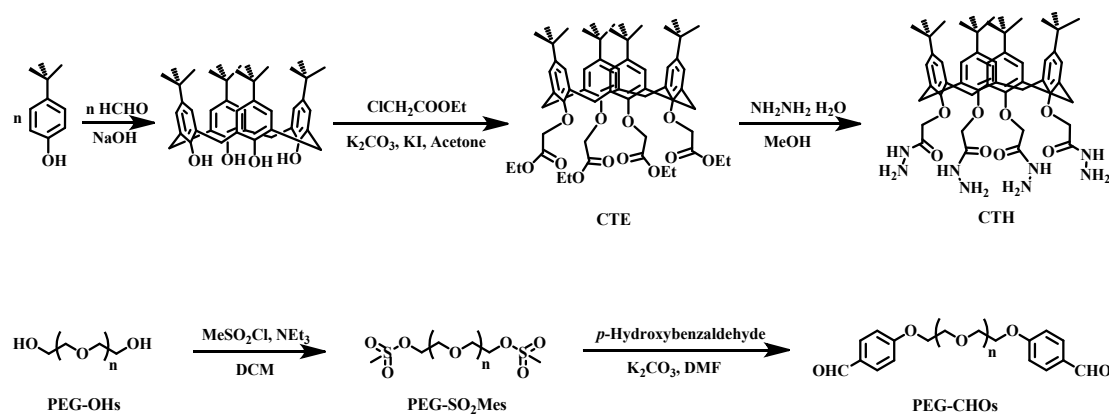
CONTENTS

1. Reagents and Materials.....	2
2. Synthetic Routes of the Reactants.....	2
3. Preparation of Ionogels.....	2
4. FTIR Measurements.....	3
5. Mechanical Tests.....	3
6. Preparation of Cathode Materials.....	3
7. Assembly of Button Battery.....	4
8. Thermal Analysis Technology.....	4
9. SEM Measurements.....	4
10. Electrochemical Impedance Spectroscopy (EIS) Measurements.....	5
11. Ionic Conductivity.....	5
12. Electronic Conductivity.....	6
13. The Li⁺ Transference Number.....	6
14. Cyclic Voltammetry.....	7
15. Constant Current Charge Discharge.....	7
16. Density Functional Theory (DFT) Calculation.....	7
17. Low Temperature Performance of the Batteries.....	8

1. Reagents and Materials

4-*tert*-Butylphenol (>98.0%) was purchased from TCI, hydrazine hydrate (80.0%) was from Guangdong Guanghua Sci-Tech Co., Ltd., *p*-hydroxybenzaldehyde was from Energy Chemical Co., Ltd., linear poly(ethylene glycol) (PEG-OHs, $M_n \sim 4000$), bistrifluoromethanesulfonimide lithium salt and propylene carbonate were from Shanghai Macklin Biochemical Co., Ltd., and ethyl chloroacetate (99.0%) and diphenyl ether (99.0%) are products of J&K Technology Co., Ltd. 1-Butyl-3-methylimidazolium tetrafluoroborate ([BMIM]BF₄, 99.0%) and propylene carbonate (PC, 97%) were from Lanzhou Green Chemistry ILs Co., Ltd. These reagents were used without further purification. Other reagents were of analytical grade and used without further purification unless otherwise specified.

2. Synthetic Routes of the Reactants



Scheme S1. The synthetic routes for CTH and PEG-CHOs.

The preparation, characterization of compounds CTH and PEG-CHOs can be consulted from our previous work (*Macromol. Rapid Commun.* **2018**, *39*, 1700679).

3. Preparation of Ionogels

The ionogels were prepared in a mixture solvent of [BMIM]BF₄ and PC without any

addition of acid-base catalyst, in which the total concentration of CTH and PEG-CHOs is 25%, w/v (nCTH : nPEG-CHOs = 1:2) and the solvent composition is 4:1 (v/v). In a typical preparation, CTH (0.0125 g) and LiTFSI (0.1435 g) were dissolved in 0.5 mL of [BMIM]BF₄/PC (4/1, v/v) at room temperature before a PEG-CHOs (0.1125 g) was added. The mixture was stirred by using a vortex mixer until the reactant was dissolved completely, and then the gels formed upon standing at ambient condition.

4. FTIR Measurements

The FTIR measurements were performed on a Bruker VERTEX70 V infrared spectrometer at room temperature. The testing scale was from 400 to 4000 cm⁻¹ with 128 scans for each sample. The KBr pellet was obtained by mixing a small amount of the sample and anhydrous KBr powder.

5. Mechanical Tests

Mechanical properties of the as prepared ionogels were measured by a Xie Qiang mechanical testing machine (CTM 2500 universal testing machine) at room temperature. In the test, all ionogels were prepared and aged for 12 hours. The ionogel specimens for the compressive tests have a cylindrical shape with 9 mm in diameter and 13 mm in height. All specimens were set on the lower plate and compressed by the upper plate at a strain rate of 2 mm/min.

The ionogel specimens for tensile tests were of a dumbbell-shape (the size of the heads: 60 mm in length, 9.0 mm in width, 1.5 mm in thickness; the size of the middle part: 40 mm in length, 5 mm in width, 1.5 mm in thickness). Besides, the uniaxially stretched tests were conducted at a constant stretching speed of 20 mm/min.

6. Preparation of Cathode Materials

LiFePO₄, acetylene black and binder polyvinylidene fluoride (PVDF) were mixed according to the mass fraction of 8:1:1. The solvent, *N*-methyl pyrrolidone (NMP), was then added and grounded in an agate mortar. The obtained slurry was uniformly coated on a fluid collector (Al foil) and placed in the oven at 80 °C for 24 h. After that, it was cut into a round sheet with a diameter of 11.4 mm by manual punching machine. The mass was weighed by an electronic balance and then put them into the glove box (H₂O < 1 ppm, O₂ < 1 ppm) for later use.

7. Assembly of Button Battery

LiFePO₄-based cathode was dried in a vacuum at 100 °C for 36 h and subsequently cut into circles (D = 11 mm), where the loading content of the LiFePO₄ is around 1.5 mg cm⁻². Lithium metal foil (battery grade) was used as the anode. To assemble a Li|Ionogel|LiFePO₄ cell, the ionogel membrane was sandwiched between the LiFePO₄ cathode and the Li anode and then packaged into a CR2025 coin cell. The whole process for the cell assembly was conducted in an argon-filled glove box.

8. Thermal Analysis Technology

Differential Scanning Calorimetry (DSC) measurements and Thermogravimetric Analysis (TGA) measurements were performed using a Q1000DSC+LNCS+FACS Q600SDT from TA Instruments. For DSC measurements, the temperature range was -80 to 80°C, and the heating rate was 10°C /min in nitrogen atmosphere. The TGA data were recorded in the heating mode at 10°C/min in nitrogen atmosphere. The temperature range was 25 to 700°C.

9. SEM Measurements

The surface morphology of the materials was analyzed using a TM 3000 Tabletop microscope (Hitachi Limited). The accelerating voltage was 15 kV and the emission current was 10.0 mA. To observe the surface morphology of the lithium metal surface after the charge and discharge cycles, the button battery which cycled 1200 times was taken apart in the glove box. Removing the anode from the battery, the ionogel electrolyte on the surface of the lithium metal was peeled off, and then cleaned with DEC. The gel electrolyte attached to the surface of the electrode was removed, and the SEM test was performed immediately after vacuum drying.

10. Electrochemical Impedance Spectroscopy (EIS) Measurements

Electrochemical impedance spectroscopy (EIS) determines the dielectric properties of materials. This is measured by the external field's interaction with the dipole moment of a particular sample, usually stated by permittivity. It is also regarded as an experimental technique that describes electrochemical systems. This method gauges system impedance over a series of frequencies. Thus, frequency response involving dissipation properties and energy storage is disclosed. Most of the time, data gathered through electrochemical impedance spectroscopy is graphically conveyed in Nyquist plots and Bode plots. In this paper, EIS was used to determine the kinetic parameters of the electrode process such as ion conductivity, lithium ion mobility and electrochemical reaction impedance of the prepared ionogel electrolyte.

All electrochemical measurements were performed on a CHI660D electrochemical workstation. The testing frequency was from 0.1~10 kHz with 5 mV of alternating current (AC) amplitude for each sample.

11. Ionic Conductivity

The testing system was assembled into a stainless steel (SS) | ionogel electrolyte | SS type blocking electrode system, and the EIS test was performed on the CHI660D electrochemical workstation. The testing system was placed in a high-low temperature alternating test chamber, and the measured temperature was -40 to 80°C. The system was set at the temperature to be measured for 30 min, so that the ionogel electrolyte reached the test temperature. Each electrolyte test was repeated 3 times and the results were averaged. The ionic conductivity (σ) of the ionogel electrolyte can be calculated according to equation 1

$$\sigma = \frac{l}{R_b \cdot S} \quad (1)$$

where l and R_b are the thickness and bulk resistance of the ionogel electrolyte under examination, respectively. S is the contact area between SS and ionogel electrolyte.

12. Electronic Conductivity

The electronic conductivity of the ionogel electrolyte was calculated through the polarization current time curve. Measurement system: SS | ionogel electrolyte | SS blocking electrode system. 1 V polarized voltage is applied to the test electrode and the change of current with time can be monitored. Under the given cell condition, the symmetric stainless steel electrode will block the Li^+ , $[\text{EMI}]^+$, and $[\text{TFSI}]^-$ ions, and only electronic flow remains constant during the whole experiment. The electronic conductivity γ can be got according to equation 2

$$\gamma = \frac{I_{SS} \cdot L}{U \cdot S} \quad (2)$$

where I_{SS} is the steady current, U is the polarization voltage, L and S are the thickness and the

area of the ionogel electrolyte.

13. The Li⁺ Transference Number

The measurement system used was Li | ionogel | Li symmetric battery, and the instrument was CHI660D electrochemical workstation. First, the battery was analyzed for AC impedance, and the initial interface resistance of electrolyte R_{ct}^0 was obtained. Then, the timing current method was used to continuously apply a certain polarization voltage ($\Delta V = 80$ mV) to both ends of the battery, and the change of current curve was recorded. When $t = 0$, positive and negative ions begin to transfer to the cathode and anode under polarization voltage, generating transient current I^0 . As time passes, anion stopped transference and gathered in the cathode, while Li⁺ can still transfer from the positive to negative under the polarization voltage. When the polarization current decay to a stable value I^s , we can consider that I^s only caused by Li⁺ transference. After stopped the polarization voltage, and the steady interface resistance R_{ct}^s of ionogel electrolyte can be obtained by analyzing EIS of the battery. In the experiment, the Bruce-Vincent-Evans equation 3 was used to calculate the transference number of Li⁺. Recent studies have shown that this method can be used for solid electrolyte system^[1]

$$t_{Li^+} = \frac{I^s(\Delta V - I^0 R_{ct}^0)}{I^0(\Delta V - I^s R_{ct}^s)} \quad (3)$$

14. Cyclic Voltammetry

CV tests were performed on a CHI660D electrochemical workstation. The test voltage was from 2.4~4.2 V and scan rate was 0.1 mV/s for each sample.

15. Constant Current Charge Discharge

In the measurements, CT2001A Land test system of WuHan JinNuo electronics co., LTD. was used to test the cycle life and multiplier performance of the battery. Voltage sweep range from 2.4 V to 4.2 V and charge-discharge rate were 0.2 C, 0.5 C, 1 C and 2 C, respectively. The Li/ionogel/LiFePO₄ half-cells were placed in a high-low temperature test chamber during the test and adjusted the temperature according to the needs of the experiment.

16. Density Functional Theory (DFT) Calculation

The energy cutoff for the plane wave basis expansion was set to 380 eV. The force on each atom was set as 0.05 eV/Å for convergence criterion. The van der Waals dispersion interaction Grimme's D3 functional was included for all models.^[2] For molecular dynamics, force field simulations were performed based on COMPASS force field,^[3] as embedded in Materials Studio.

Before running MD, the geometries have been fully optimized, followed by NVT dynamics simulation at $T=243$ K, 273 K and 303 K. In all cases, simulation was made with a time step of 1 fs, running for a whole length of 500 ps.

17. Low Temperature Performance of the Batteries

More specially, the button battery has an operating voltage of 3.4 V, which was high enough to power a yellow LED at ultra-low temperatures. Of course, as the temperature decreases, the performance of the battery was declined synchronously, and the brightness of the LED gradually weakened. The LED starts to turn on again while the temperature rises (**Figure S13**) which shows that the extremely low temperature will exactly affect the battery performance, but it is not permanent damage. The particular property of this battery maybe plays a big role in an emergency although it does not seem to be sustainable.

Figures:

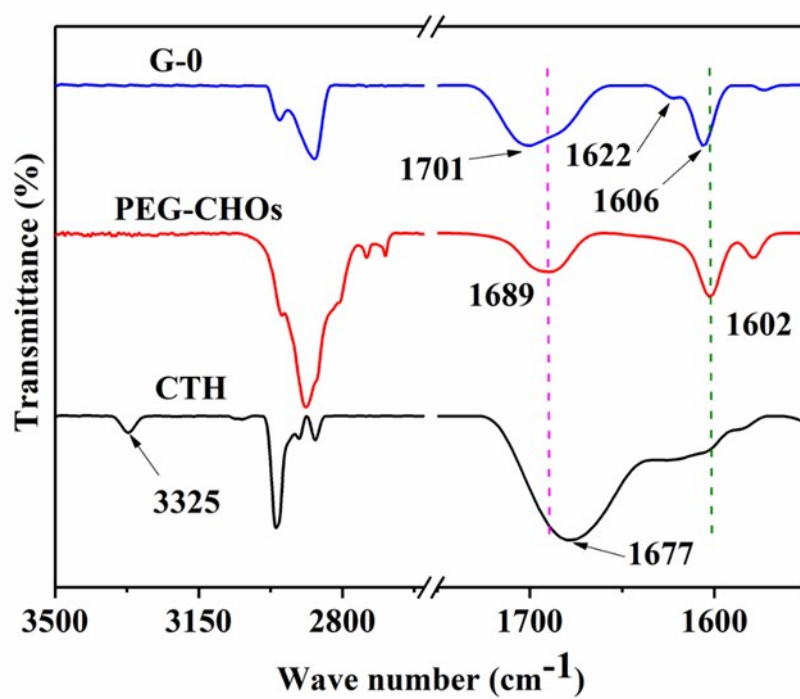


Fig. S1 FTIR spectra of CTH, PEG-CHOs and ionogel (freeze-dried)

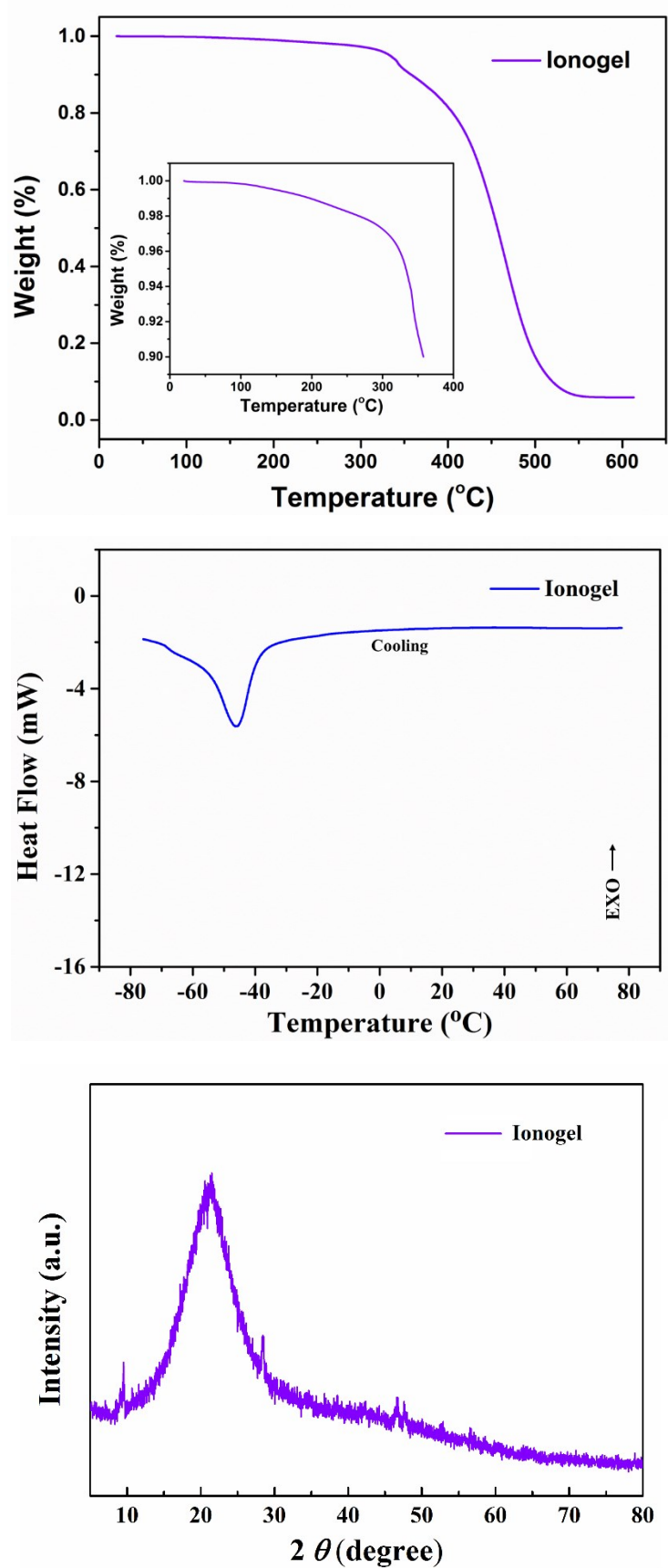


Fig. S2 (a) TGA, (b) DSC and (c) XRD curves of the as prepared ionogel.

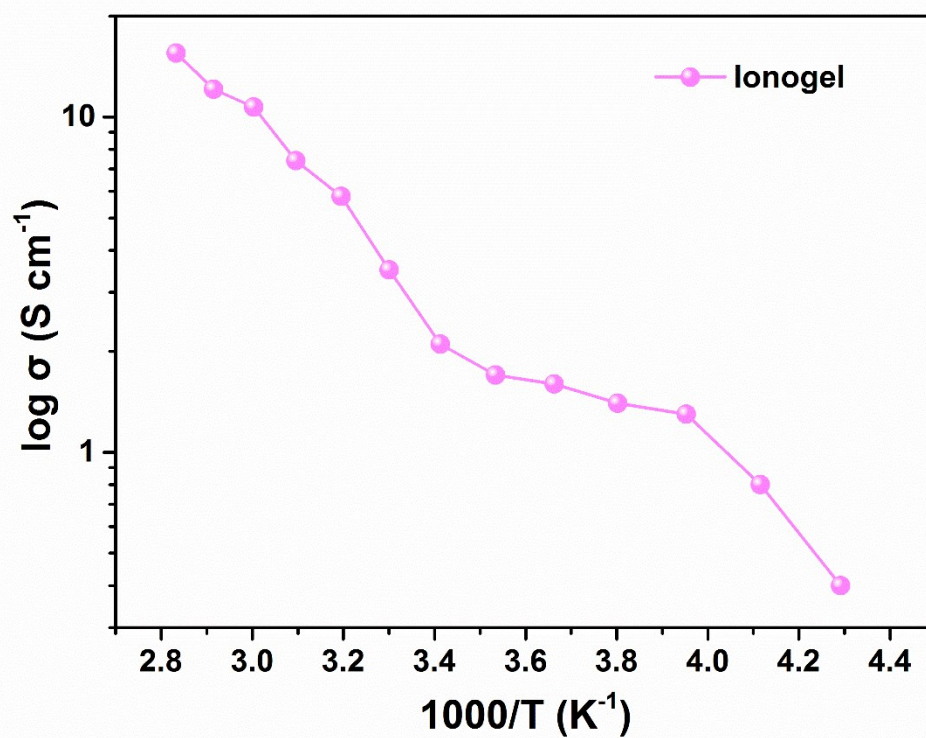


Fig. S3 Ionic conductivity of the ionogel-based battery at different temperatures.

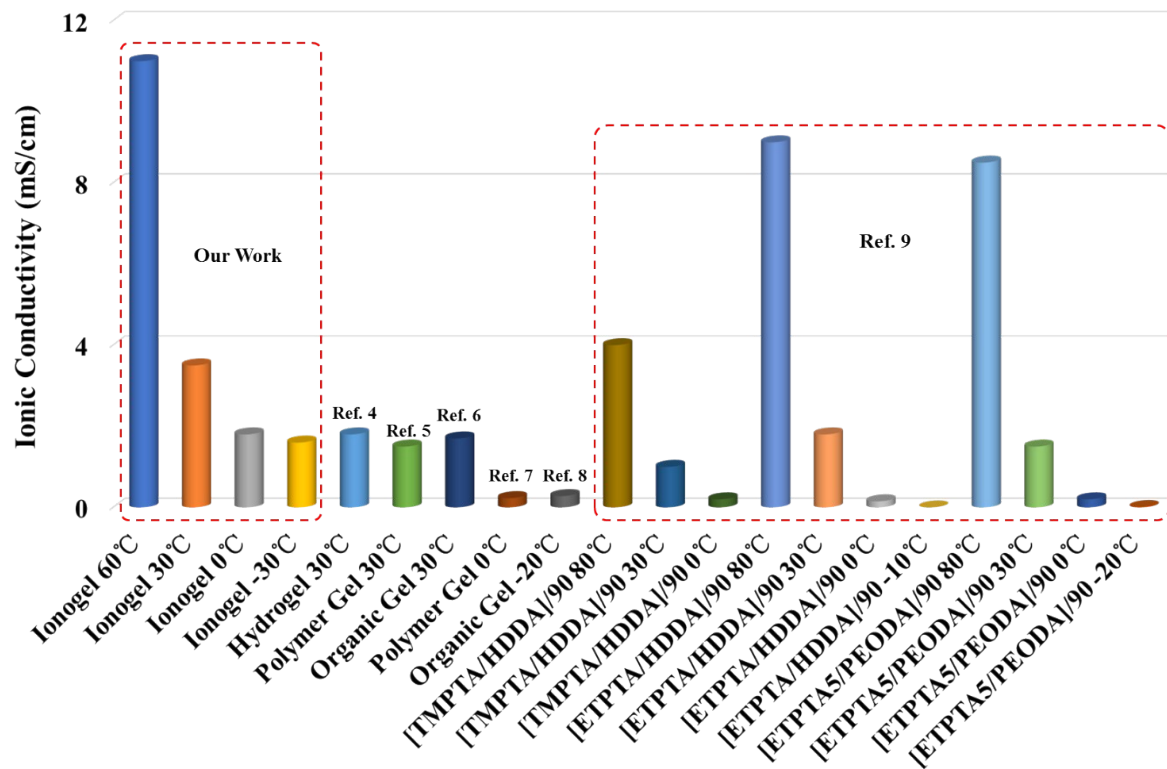


Fig. S4 Comparison of ionic conductivity for present and other gel electrolytes.

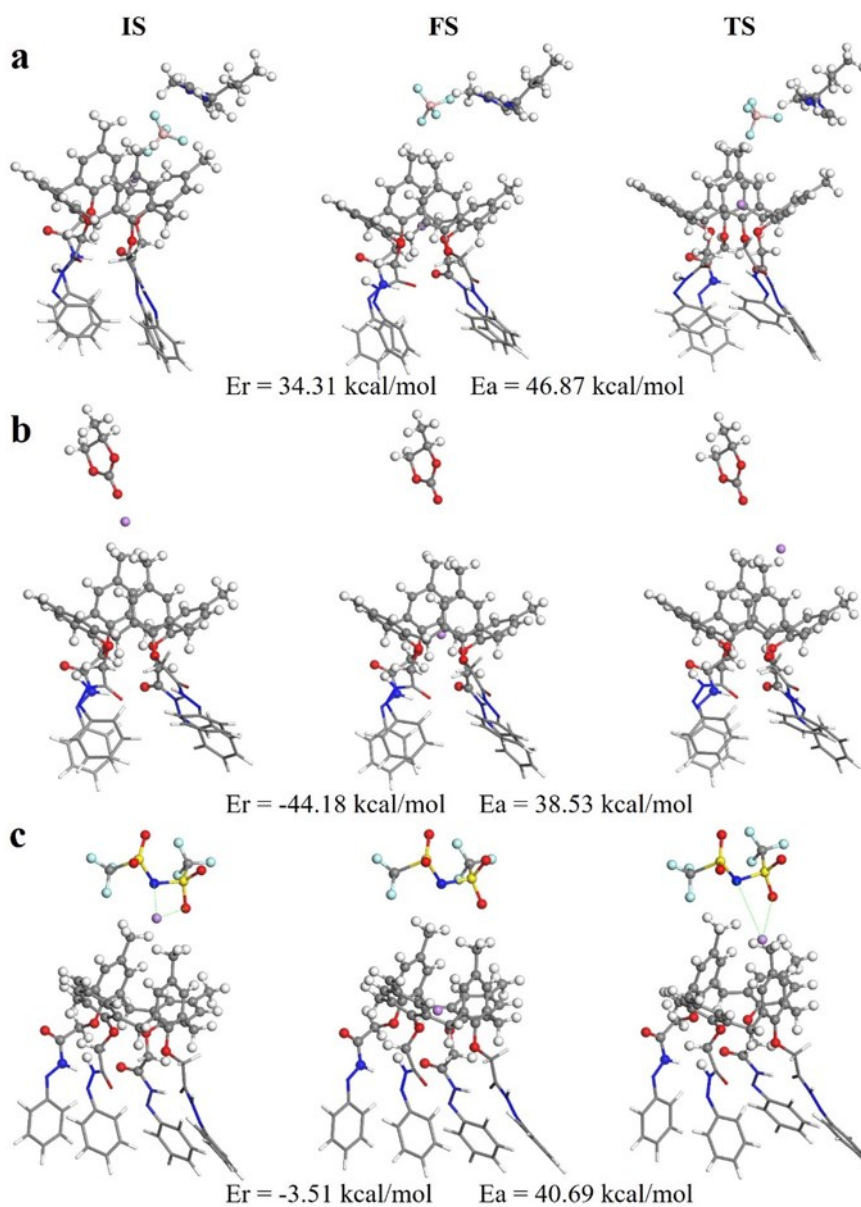


Fig. S5 Calculation of the lithium ion de-solvation and entering the cavity of CTH in the presence of different additives. (a) [BMIM]BF₄; (b) PC; (c) LiTFSI. *Note:* IS: initial state; FS: final state; TS: transition state. E_r stands for reaction energy (the energy for trapping Li⁺ from the ionic liquid), and E_a stands for activation energy (the energy for Li⁺ leaving from the host, CTH).

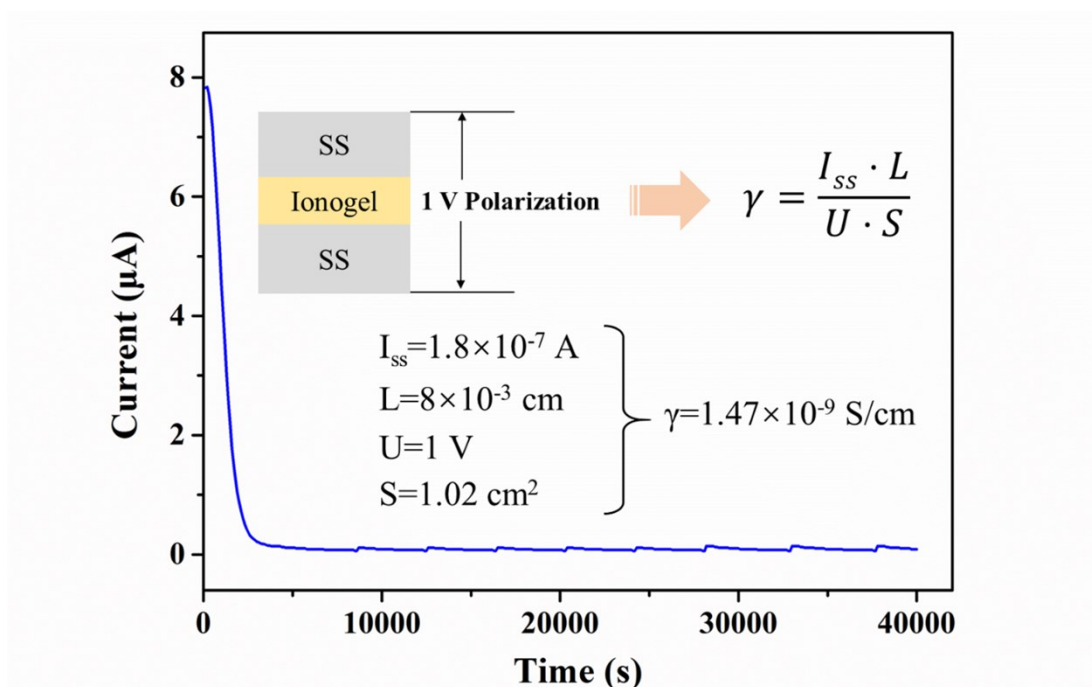


Fig. S6 Current-time profile of the SS/ ionogel /SS cell obtained by adding a polarization voltage of 1 V at room temperature.

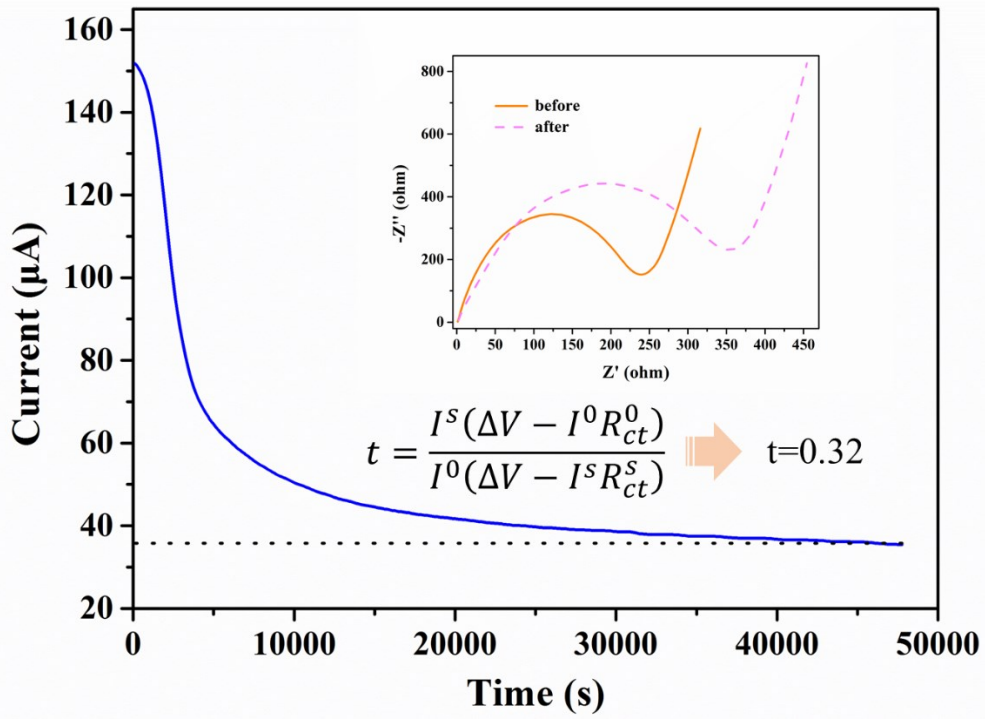


Fig. S7 Transference number for the as prepared ionogel at room temperature. Inset: Impedance response of the cell before and after the dc polarization

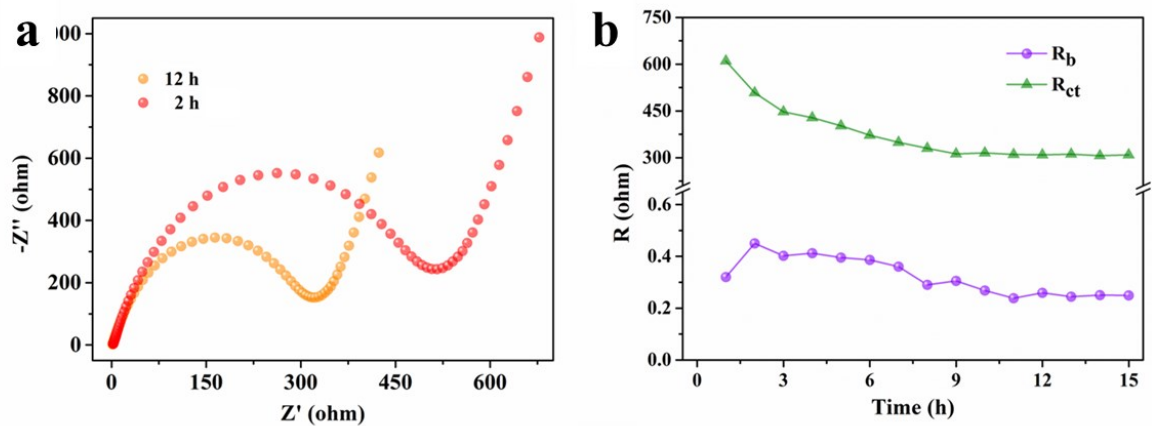


Fig. S8 (a) Time evolution of the impedance response of a symmetrical Li/ionogel/Li cell at room temperature; (b) Bulk (R_b) and interfacial (R_{ct}) impedances at room temperature as a function of time.

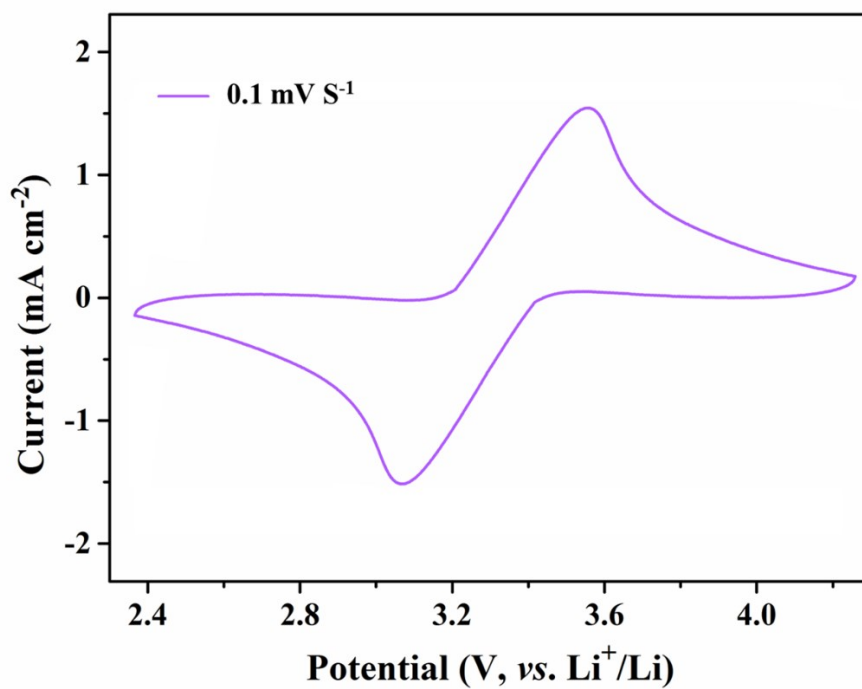


Fig. S9 Cyclic voltammogram of the Li/Ionogel/LiFePO₄ cell at 0.1 mV S⁻¹.
Voltage range: 2.4-4.2 V

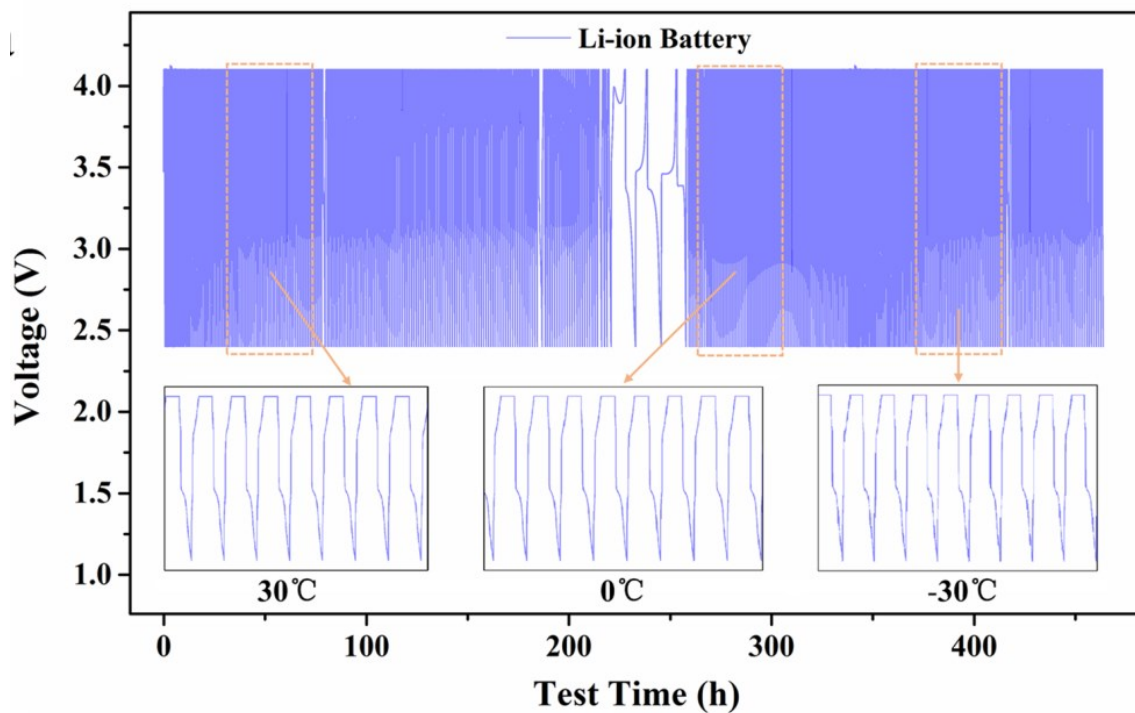


Fig. S10 Voltage profiles of Li metal battery along with cyclic cooling and heating process at 0.2 C.

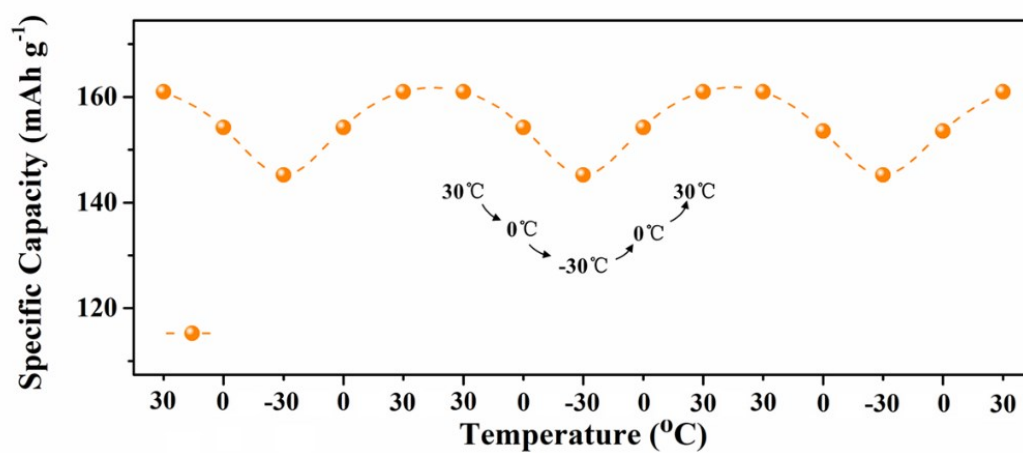


Fig. S11 Cyclic testing of ionogel battery under 30, 0, -30 °C at 0.2C.

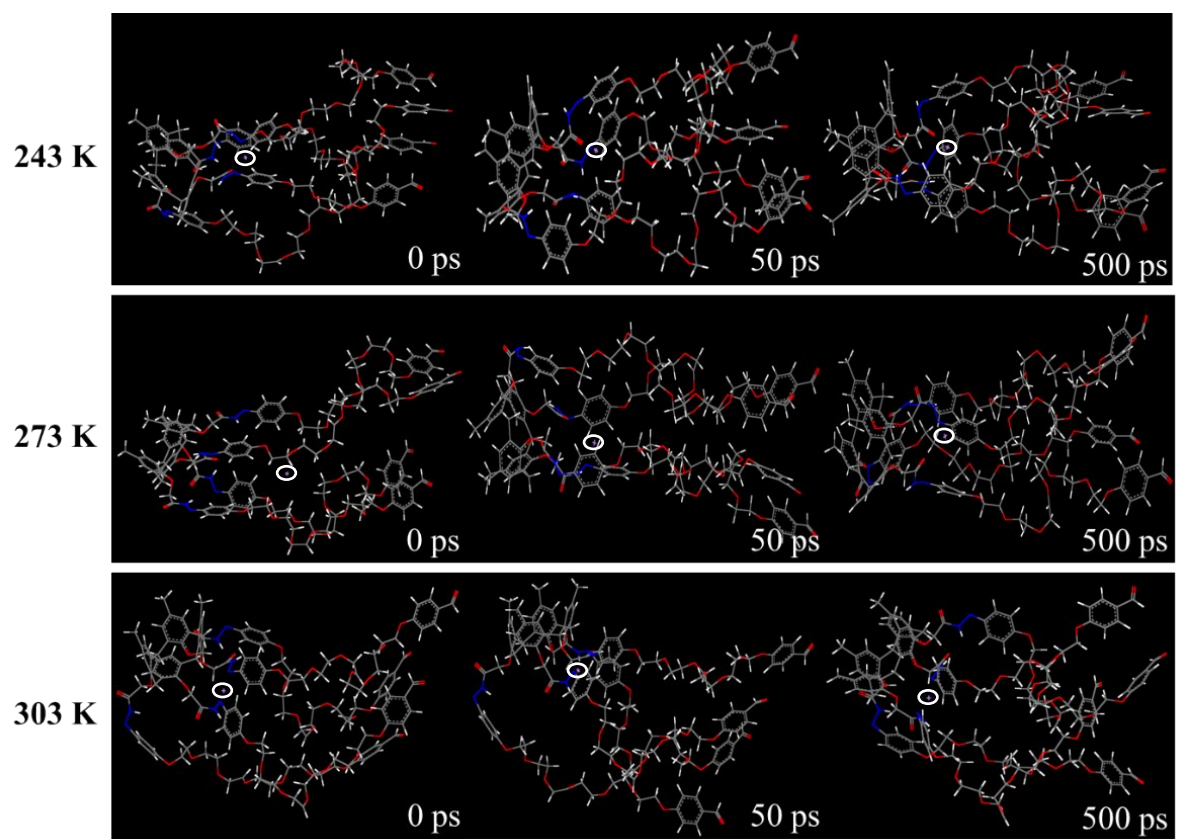


Fig. S12 Li^+ transference on the polymer chains from 0 to 500 ps.

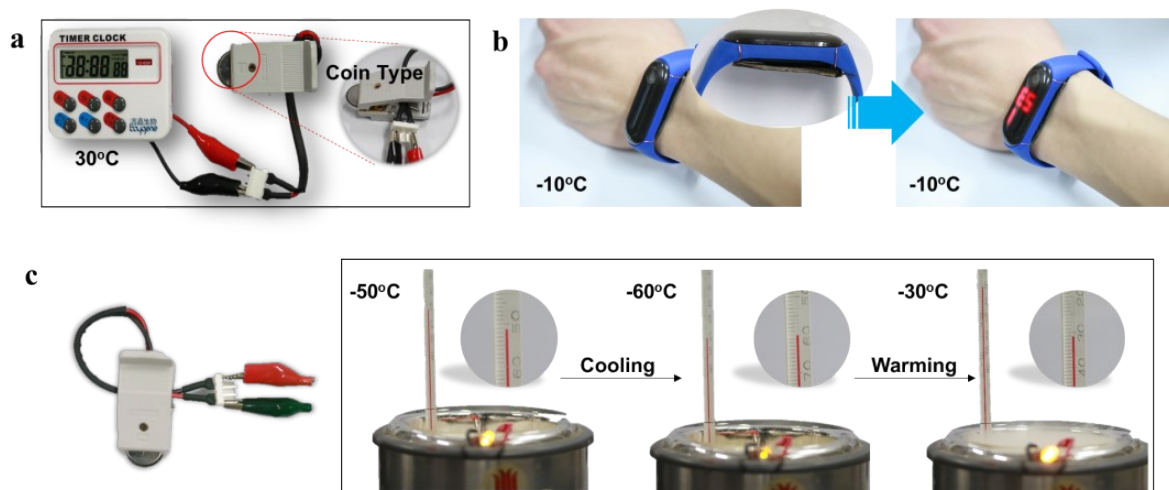


Fig. S13 (a) Room temperature performance of the coin-type battery. (b) The flexible battery powering wearable electronics at -10°C . (c) The coin-type battery could power a yellow LED even at -50°C and -60°C . At the same time, the LED became brighter with the temperature returning to -30°C .

References

- [1] Y. Mo, L. Song and Y. Lin. *J. Phys. Chem. A*, **2007**, *111*, 8291.
- [2] F. Wu, N. Chen, R. Chen, Q. Zhu, J. Qian and L. Li. *Chem. Mater.* **2016**, *28*, 848.
- [3] H. Sun, *J. Phys. Chem. B*, **1998**, *102*, 7338.
- [4] Q. Tu, L. Fan, Fei Pan, J. Huang, Y. Gu, J. Lin, M. Huang, Y. Huang and J. Wu. *Electrochimica Acta*, **2018**, *268*, 562.
- [5] S. Chen, B. Zhang, N. Zhang, F. Ge, B. Zhang, X. Wang and J. Song. *ACS Appl. Mater. Interfaces*, **2018**, *10*, 5871.
- [6] M. Yao, D. Su, W. Wang, X. Chen and Z. Shao. *ACS Appl. Mater. Interfaces*, **2018**, *10*, 38466.
- [7] K. Shikinaka, N. Taki, K. Kaneda and Y. Tominaga. *Chem. Commun.*, **2017**, *53*, 613.
- [8] D. Nandakumar, J. V. Vaghasiya, L. Suresh, T. Duong and S. Tan, *Mater. Today Energy*, **2020**, *17*, 100428

- [9] D. Aidoud, D. Bouyssou, D. Guyomard, J. Bideau and B. Lestriez. *J. Electrochem. Soc.*, **2018**, *165*, A3179.